NASA CR-66978

ATMOSPHERIC AND OCEANOGRAPHIC SUPPORT STUDIES FOR LASER RADAR EXPERIMENT ABOARD THE ADVANCE II DURING BOMEX

Prepared for

National Aeronautics and Space Administration
Langley Research Center
Hampton, Virginia

August 1970

(Prepared under Contract NAS1-9161 by the
Engineering and Environmental Sciences Division of the
Research Triangle Institute, Research Triangle Park
North Carolina)

ATMOSPHERIC AND OCEANOGRAPHIC SUPPORT STUDIES FOR LASER RADAR EXPERIMENT ABOARD THE ADVANCE II DURING BOMEX

By Walter D. Bach, Jr.
and James R. Smith

Prepared under Contract NAS1-9161 by
RESEARCH TRIANGLE INSTITUTE
Research Triangle Park, N. C.

for

NATIONAL AERONAUTICS AND SPACE ADMINISTRATION

ABSTRACT

During June and July, 1969, the NASA optical radar was aboard the S. S. ADVANCE II on a cruise from Wilmington, North Carolina through the BOMEX area and to the mouth of the Amazon River. During that cruise over 800 laser firings were made to investigate the features of the marine atmosphere and to evaluate the performance of the laser within a marine environment. Frequent radiosonde releases were made to provide data on the thermal and moisture structure of the atmosphere.

Analyses of both high altitude (>15 km) and low altitude (>3 km) laser data were made for one of the observing stations. The presence of dust layers between 15 and 25 km was verified. Short term changes in dust concentrations and the laser profile characteristics were noted. Data obtained by varying the elevation angle of the laser and firing at approximately one-minute intervals permitted the construction of space cross sections through the planetary boundary layer. The resulting distributions show characteristics of a dry convective regime having the dimensions and other properties of fair weather cumulus clouds. Estimates of vertical velocities in the clouds were made.

The intertropical convergence zone was located by an air trajectory analysis. Measurements of particle number density to the south of that zone showed an order of magnitude decrease in large (>1μ) particles from measured number densities to the north of the zone.

FOREWORD

This report was prepared by members of the Engineering and Environmental Sciences Division of the Research Triangle Institute (RTI), Research Triangle Park, North Carolina under Contract No. NAS1-9161.

The work was sponsored by the National Aeronautics and Space Administration, Langley Research Center, Instrument Research Division. Dr. J. D. Lawrence was the NASA Technical Representative for this study.

The Project Director was Mr. James R. Smith, who was also RTI's chief scientist aboard the S. S. ADVANCE II. Dr. Lawrence and other NASA scientists conducted the laser firings aboard ship and have reduced laser data into digital form. The meteorological and laser data analysis included herein was performed by Dr. Walter D. Bach, Jr. of RTI.

Special acknowledgement is made to Messrs. Lloyd Chamberlain, Paul Murphy, and Bob Mullins of ESSA, Wallops Island, Virginia, who operated the radiosonde system and reduced that data in addition to making and recording the regular weather observations. Captain Arthur W. Jordan and the crew of the S. S. ADVANCE II, and the students from the Cape Fear Technical Institute, Wilmington, North Carolina deserve special acknowledgement for their cooperation and assistance throughout the cruise.

TABLE OF CONTENTS

LIST OF FIGURES

LIST OF TABLES

ATMOSPHERIC AND OCEANOGRAPHIC SUPPORT STUDIES FOR LASER RADAR EXPERIMENT ABOARD THE ADVANCE II DURING BOMEX

Walter D. Bach, Jr. and James R. Smith
Research Triangle Institute

INTRODUCTION

An optical radar system has the particular capability to transmit a large amount of monochromatic light energy in a short pulse in a collimated beam. The system can detect scattering within clear (as opposed to liquid water clouds) air by the air molecules and by the aerosols present. Unique detection of those scatterers is not possible with conventional (microwave) radar. Consequently, optical radar systems have been used in investigations of smoke plumes in air pollution studies (ref. 1), in studies of the onset of fog or stratus (ref. 2) and the so-called 20 km dust layer (refs. 3,4,5) among others. In most of these studies, it was necessary to carry out a meteorological measurement program to assess the structure and changes in structure which accompany the changes detected by the laser.

Large amounts of dust have been collected on the eastern extremity of the island of Barbados (ref. 6). The dust was determined to be of African origin, transported westward by the persistent northeast trade winds. In addition to the dust, salt nuclei resulting from evaporation of sea spray are abundant in the marine environment.

High intensity searchlight beams have been used to study the scattering of light within the atmosphere (ref. 7). The presence of a dust layer near 20 km has been a persistent result of those studies. Junge, Chagnon, and Manson (ref. 8) have sampled concentrations in that region directly from aircraft. Rosen (ref. 9) has used a balloon-borne particle size distribution measuring device to sample the layer. He also found that the layer was higher near 10°N (~20 km) than near 60°N (~12 km). Two sources of the dust are postulated to be volcanoes and tropospheric dust raised aloft by deep convection in the tropics near the intertropical convergence zone and carried northward by the circulation systems aloft.

The Research Triangle Institute (RTI) conducted a cruise aboard the S. S. ADVANCE II as a part of the Barbados Oceanographic and Meteorological Experiment (BOMEX) (Fig. 1). The principle experiment conducted on the cruise was the probing of all levels of the marine atmosphere using the NASA-Langley Research Center (LRC) optical radar system, which was operated by NASA-LRC scientists. Radiosonde releases were made at appropriate intervals to determine the thermal and moisture structure of the atmosphere. A particle size sampler was also aboard the ship to provide information on the aerosol distribution near the sea surface.

Figure 1.

COURSE OF SS ADVANCE II THROUGH BOMEX STUDY AREA FROM WILMINGTON, N.C., TO AMAZON RIVER, JUNE - JULY 1969.

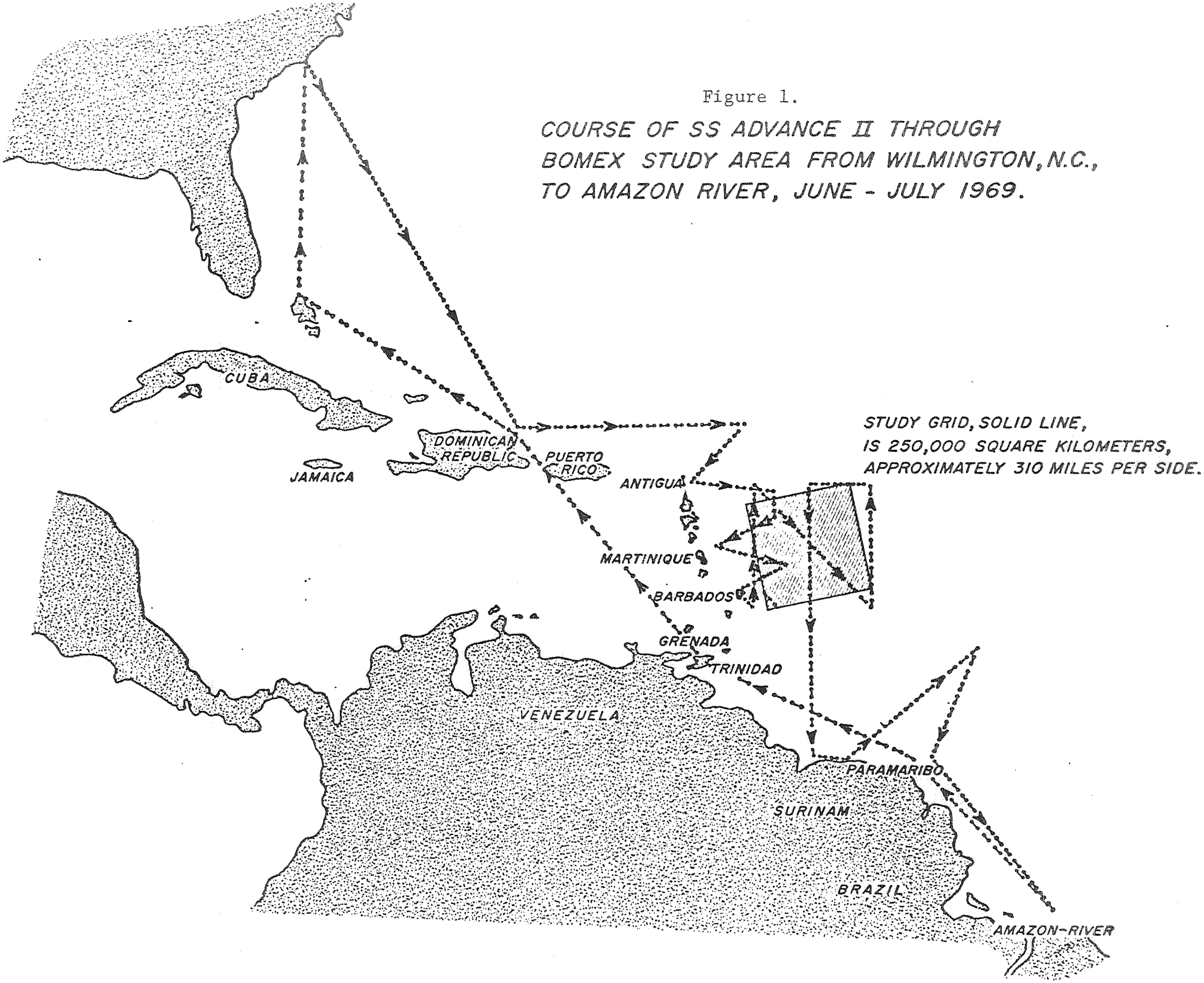

DATA ACQUISITION

Laser Data Acquisition

It is beyond the scope of this report to examine the details of the operation of the optical radar system. That has been done by Lawrence, Crownfield, and McCormick (ref. 10). It is, however, pertinent to examine the principles of the system and the manner in which the data were derived.

In principle, the operation of the laser system is relatively simple. A pulse of collimated, monochromatic light (6943 Å wavelength) is transmitted in a short burst. That light is partially absorbed, scattered, and transmitted through the atmosphere. Some of the scattered light is returned to the system receiver where it is collected, amplified, converted to an electric potential. In the system used, the voltage, V, is eventually displayed on a dual-beam cathode ray oscilloscope (CRO) as a function of the time, t, which has elapsed since the pulse was transmitted. The CRO image is preserved for later analysis by automatically taking a Polaroid picture of the display. The magnitude of V due to scattering at a range, R, is given by

$$V = ecE\, q^2\sigma/2R^2 \tag{1}$$

where

- e is the efficiency of the receiver system,
- c is the speed of light (assumed constant),
- E is the laser energy,
- q is the one-way extinction coefficient,
- σ is the volume backscatter cross section at R,

and

$$R = ct/2. \tag{2}$$

All of the parameters in Eq. (1) can be measured or are known by calibration except the atmospheric terms q and σ, and the system efficiency. Consequently

$$q^2\sigma \propto VR^2(2/eEc) \tag{3}$$

represents the total relative backscatter from the given range. It is this quantity as a function of R that is used as a measure of the atmospheric properties. Unfortunately, $q^2\sigma$ is dependent upon the processes of extinction and scattering which occurs at lesser ranges as well as at R. Consequently, absolute values cannot be ascribed to the measurement. Although $q^2\sigma$ values are not corrected for attenuation they do represent a lower limit for the scattering and, to a large extent, it may be possible to relate their changes between adjacent ranges to atmospheric changes.

The scattering of the beam is due to molecules of air and aerosols such as dust, water drops, ice crystals, etc. As the molecular sizes are much less than the wavelength of the radiation, Rayleigh scattering theory applies to the molecular scattering. The number density of molecules at a given height in the atmosphere is relatively constant in time and space, so the contribution of Rayleigh scattering to the total scattering can be estimated reasonably well. Hence the Mie scattering due to aerosols can be estimated from the returned signal. Further analysis, taking into account the range and the intervening aerosols and molecules can give estimates of the integrated backscatter cross sections of the aerosols in a given layer.

Aboard ship, the laser was operated in two principal modes. Primarily it was pointed normal to the horizon plane. A gyro stabilization system prevented the laser from firing when the ship was tilted more than 5° from the horizontal. Less than a millisecond is required between firing and signal reception at maximum range so no significant error is induced by the ship's roll or pitch. In that configuration, vertical profiles of scattered radiation could be obtained. For high resolution in a given altitude range, the return signal could be gated so that only a portion of the entire returned signal was displayed on the CRO. The sweep time (abscissa) and sensitivity (ordinate) of the CRO beams could also be independently varied in order to get high and low resolution within a layer. All of this information was recorded with each photograph. This mode of operation was restricted to times of very low sun elevation angle and/or nighttime in order to prevent detection of scattered or direct sunlight.

The second mode of operation was to fire the laser at various elevation angles at approximately one-minute intervals. The objective of this mode is the examination of spatial and/or temporal variations of the atmospheric boundary layer. By probing that layer, it was hoped that it would be possible to define incipient thermals or plumes that precede the formation of visible clouds, to find indicators of turbulent mixing, and to observe the trade wind inversion.

In either mode, it was necessary to use neutral density filters to reduce the returned signal to prevent saturation of the electronics system. At low altitudes (<3 km) the filter used reduced the back-scattered energy by three orders of magnitude. As the altitude of interest increased, less dense filters were used. The effect of the filter is incorporated in the efficiency term, e, of Eq. (1). After setting up at a sampling station, the usual procedure was to make several vertical probes to determine the basic features of the atmosphere. Then further probes of the altitudes of the interesting features were made.

Upon completion of the cruise, the analysis of the approximately 800 laser probes was initiated by NASA scientists. The mechanics of data reduction and verification were quite tedious and time consuming. Many features of interest could be identified from individual photographs, but until the final data reduction was completed, no discrete numbers could be applied for analysis.

Meteorological Data Acquisition

In conjunction with the optical radar probing of the atmosphere, the thermal and moisture structure of the air was determined using the U. S. Weather Bureau portable radiosonde system, located aboard the ADVANCE II. Soundings were made at appropriate time intervals to define the synoptic scale of changes, but were not made for each series of laser firings. Thirty-one radiosonde releases were made from the ADVANCE II in support of the optical radar program. Due to the nature of the system and the shipboard operation, it was not possible to get wind velocities from the drift of the balloon.

Within the BOMEX area, radiosonde soundings from the ADVANCE II were not made. Comprehensive data on the short term variability of the atmospheric structure were collected by instrumentation aboard the permanent ships and by frequent radiosondes released from them. The lack of radiosonde data from the ADVANCE II was not considered to be detrimental in that portion of the cruise.

In addition to the radiosondes, three-hourly ship weather observations were made and recorded while at sea. These observations include cloud type, amount, and heights, visibility, obstructions to visibility, wind velocity, air temperature, pressure, dew-point temperature, sea temperature, wave height, and wave period. Hourly observations of wind velocity, air temperature, and sea temperature were also made and recorded.

All of the above data were available in reduced or coded form soon after the completion of the cruise. Auxiliary data have been obtained from the National Hurricane Research Laboratory (NHRL) and the BOMEX analysis office (BOMAP). The former source routinely prepares and analyzes maps of standard meteorological pressure levels using all available data, covering at least the area from 0 to 120°W longitude and 0 to 45°N latitude. The latter source had the unchecked radiosonde data from the USC&GS ships DISCOVERER (17°40'N 54°45'W) and OCEANOGRAPHER (13°00'N 53°47'W) and the USCG Cutter ROCKAWAY (14°30'N 56°30'W) at 0000 and 1200 GMT which were available. To date, the remaining observations are not processed or otherwise available for analysis.

DATA ANALYSIS

Laser Data Analysis

The time required to digitize and check the laser data taken on the cruise prevented a comprehensive survey of all of the data. Instead, to meet the objectives of the research, NASA and RTI scientists decided to investigate a limited amount of data in as much detail as time permitted.

The sequence of laser firings made at 14°00'N latitude 56°29'W longitude from 2330 GCT, 26 June to 0019 GCT, 27 June were chosen for study because:

(1) they were considered to be representative of conditions which were encountered in the BOMEX area;

(2) the data were "good";

(3) all altitude ranges were included in the data; and

(4) slant range probes of the boundary layer were made.

The weather observation aboard ship at 27/0000 GCT showed two-tenths sky coverage by fair weather cumulus clouds whose bases were estimated to be at 500 m. A cloud top height was not reported. No higher clouds were reported. The wind was from 080° at 8 knots. Visibility was 20 km. Wave height and period were 1.5 m and 6 sec, respectively. The ship's heading was 190° with some variation. These conditions were considered very favorable for laser operations and for investigating all altitudes.

Even when this set of data was chosen, it was known that all permanent ships of the BOMEX array were in port for re-supply and recalibration of instruments on 27 June. The ADVANCE II position was nearest to the position taken by the ROCKAWAY and data for 1200 GCT 26 June were readily available. It was hoped that later data--a special radiosonde from the ROCKAWAY--would be available in time to include in this analysis. It was not. Thus, the 1200 GCT radiosonde was used as an estimate of the atmospheric structure.

Twenty-five (25) different laser firings were made. Pertinent information on each firing is given in Table 1. Of particular interest were the values of $q^2\sigma$, the total relative backscattering volume, as a function of altitude, z.

Sources of Error.--One of the principle problems which is always encountered in data analysis is that of separation of signal and noise. The basic electronics system has shown a high signal-to-noise ratio for operations below 30 km. However, noise is introduced in the CRO display and the reduction of data from the Polaroid picture.

Letting δ be the uncertainty in the voltage, ε the uncertainty in R, and γ the uncertainty in the laser energy E, the fractional error in $q^2\sigma$ is given by

$$\alpha = \delta/V + 2\ \varepsilon/R - \gamma/E \ . \qquad (4)$$

The voltage decreases with increasing range. Therefore the fractional error due to error in voltage readings will increase with

TABLE 1

LASER PARAMETERS FOR ANALYZED OBSERVATIONS

Record Number Record	Time (GCT)	Laser Elevation Angle (degrees)	Altitude		Laser Energy (joules)	Neutral Density Filter
			Minimum (m)	Maximum (m)		
402-1	26/2324	90	1,120	3,273	1.0	3
-2			1,239	3,746		
403-1	2325	90	1,072	3,521	1.0	3
-2			1,527	3,592		
404			NO	DATA		
405-1	2329	90	3,137	7,381	1.2	2
-2			3,896	9,633		
406-1	2330	90	5,195	14,536	1.3	1
-2			8,241	19,403		
407-1	2332	90	5,402	13,986	0.9	1
-2			7,707	17,986		
408-1	2336	90	14,506	29,496	1.1	0
-2			18,853	28,850		
409-1	2337	90	12,942	28,810	1.3	0
-2			15,782	27,049		
410-1	2340	90	11,419	28,790	1.2	0
-2			12,922	25,133		
411-1	2342	90	11,570	28,638	1.2	0
-2			13,124	25,234		
412-1	2345	90	19,085	28,628	0.9	0
-2			19,085	30,726		
413-1	2347	90	19,085	28,759	1.0	0
-2			20,266	27,907		
414-1	2349	90	17,552	29,385	1.0	0
-2			20,604	28,068		
415-1	2352	90	17,542	28,204	0.8	0
-2			19,277	31,836		
416-1	2355	90	14,879	27,105	1.1	0
-2			20,503	26,913		

-1 indicates upper CRO trace.
-2 indicates lower CRO trace.

TABLE 1. — Concluded

LASER PARAMETERS FOR ANALYZED OBSERVATIONS

Record Number	Time (GCT)	Laser Elevation Angle (degrees)	Altitude		Laser Energy (joules)	Neutral Density Filter
			Minimum (m)	Maximum (m)		
417-1	26/2357	90	13,013	26,671	0.8	0
-2			15,812	26,126		
418-1	2359	90	10,037	27,962	0.7	0
-2			11,848	23,443		
419-1	27/0003	90	1,021	7,334	0.5	3
-2			1,165	8,231		
420			NO	DATA		
421-1	0006	90	1,082	2,121	0.6	3
-2			1,100	2,055		
422-1	0007	90	1,024	3,432	0.8	3
-2			1,397	3,591		
423-1	0009	67.5	960	3,334	1.0	3
-2			1,476	3,449		
424-1	0010	45	849	2,448	0.7	3
-2			1,053	2,600		
425-1	0012	22.5	446	1,311	0.8	3
-2			697	1,326		
426-1	0014	45	881	2,247	0.6	3
-2			1,056	2,628		
427-1	0015	22.5	450	1,348	0.6	3
-2			746	1,405		
428-1	0017	33.8	642	1,728	0.7	3
-2			1,004	1,807		
429-1	0019	90	1,042	3,314	0.8	3
			1,336	3,614		

-1 indicates upper CRO trace.
-2 indicates lower CRO trace.

increased range regardless of the actual range. At low altitudes, there may be some contribution to α by ε but this error source is reduced with increasing range.

If the error in reading the ordinate and abscissa is of the order of the CRO trace width (~0.04 cm), δ and ε for a trace can be obtained from the sweep and sensitivity characteristics of the CRO. An estimate of the maximum value of α at the third and third from last ranges for the upper and lower traces for a low and a high altitude probe has been made from available data. The calculations are summarized in Table 2, assuming that $\gamma = 0.05$, since the laser data were given to the nearest tenth of a joule.

The values of α are of course high for the higher altitudes of the low sensitivity (upper trace) measurements. The listed values of α are the maximum possible due to reading error only.

A check on the actual error for a given laser firing can be made by comparing the slopes of the upper and lower trace. Where they are substantially different, the slope of the lower trace should be accepted as being more realistic. Where the slopes are similar, it can be assumed that the reduced data are accurate, although the magnitude of $q^2\sigma$ may be different at the same altitude. All data presented in this report were visually checked for accuracy in this manner.

High Altitude Analysis.--The basic objective of this analysis was to identify, if possible, the so-called 20 km dust layer. Rosen's data from direct particle size sampling over Panama (ref. 9) show three well defined peaks in the dust concentration at 17, 20, and 22 km. Each peak is contained in a 1-km thick layer. The 20-km peak shows the largest dust concentration and no substantial changes fifty hours later. The upper and lower peaks had a 50 percent decrease in magnitude but remained at the same altitude.

If the air is free of dust, $q^2\sigma$ will decrease exponentially with height in the 15 to 25-km region of the atmosphere. When a layer of dust is encountered by a laser beam, more energy will be returned to the receiver. The slope of $q^2\sigma$ vs range increases in magnitude. Within a dust layer, the magnitude of $q^2\sigma$ will remain approximately constant. The top of the dust layer should be identifiable by a greater than logarithmic decrease of $q^2\sigma$. Lawrence, et al. (ref. 4) identify the 20-km dust layer in such a manner.

The high altitude (15 to 25 km) data, obtained from Records 408 to 418 were plotted as a function of altitude and time to show the slope and changes of slope which take place in each record as well as the time continuity of similar features. (See Fig. 2)

TABLE 2

ERRORS IN REDUCING LASER DATA

Record Number	Laser Energy (j)	Sweep μ sec/cm	Sensitivity mv/cm	ε (km)	δ (mv)	R (km)	V (mv)	$q^2\sigma$ (arbitrary units)	α_{max} percent
422-1	0.8	5	50	0.030	2	1.072 3.094	79 8	114. 90.6	14 33
422-2	0.8	5	10	0.030	0.4	1.506 3.304	54 4	154. 55.6	11 18
410-1	1.2	20	100	0.120	8	11.913 25.612	341 16	40.3 9.0	8 54
410-2	1.2	10	50	0.060	2	13.189 23.423	261 29	37.8 13.1	2 12

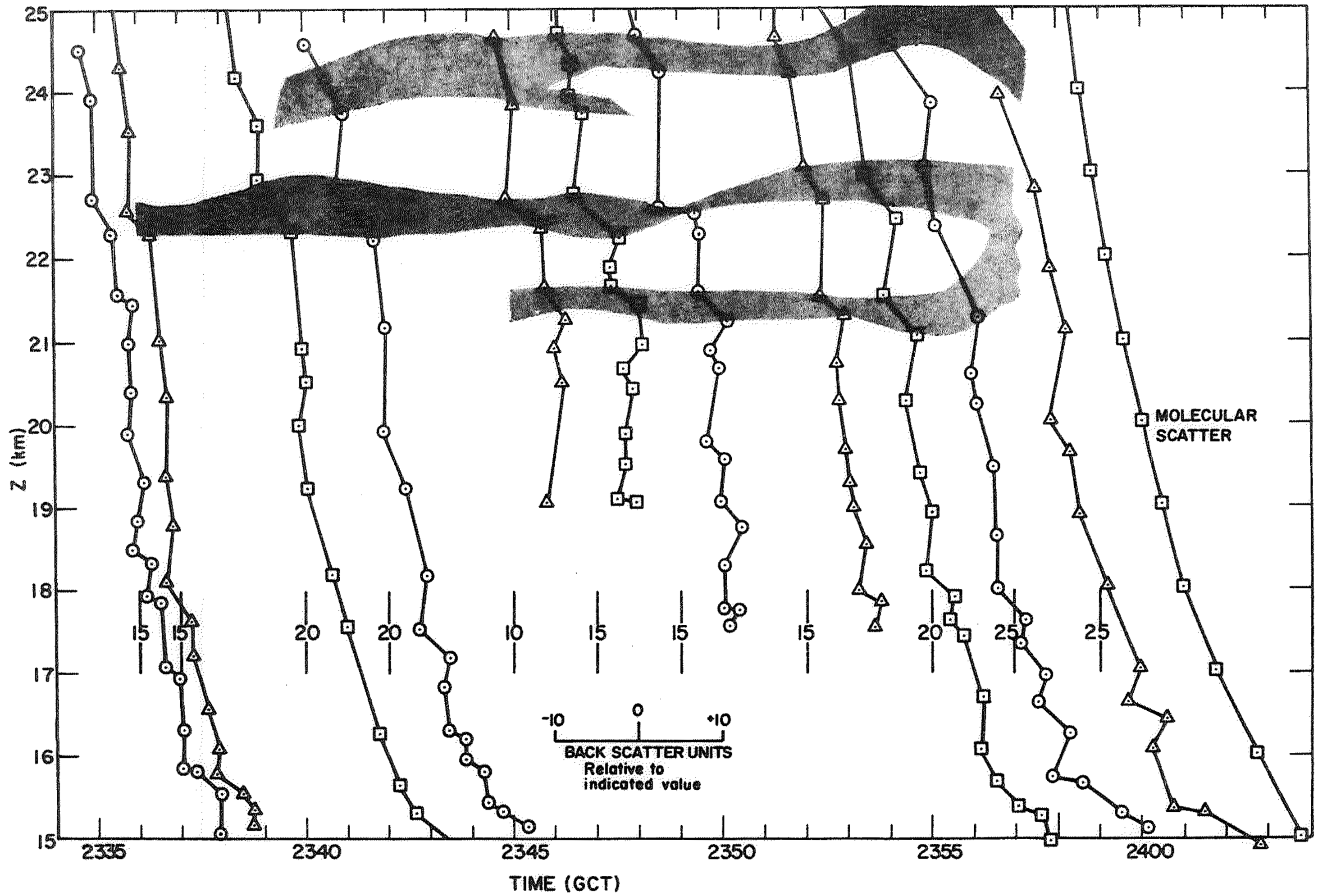

Figure 2. Time cross section showing profiles of $q^2\sigma$ vs. altitude. Continuous regions of rapid decrease with height are shaded. Molecular scatter profile is for a dust-free atmosphere.

The profile of $q^2\sigma$ anticipated from a dust-free, U. S. Standard Atmosphere (1962), using the same laser system is also given in that figure. That profile is included to assist in the identification of departures of slope from a purely molecular scattering profile.

The magnitude of $q^2\sigma$ at a given altitude is not always the same, due to varying amounts of attenuation by the lower atmosphere. The vertical lines placed between 17 and 18 km indicate the time (to the nearest minute) that the profile which first crosses that line above 17 km was taken. The number accompanying the vertical line is the value of $q^2\sigma$ at the altitude where the profile crosses the line. The scale of units in the center of the figure is the scale for changes in $q^2\sigma$.

The most persistent feature of Fig. 2 is the layer beginning about 22.4 km, 300 to 600 m thick, where $q^2\sigma$ decreases rapidly (middle shaded layer). The presence of dust below that layer is indicated by the increase or only slight decrease of $q^2\sigma$ with increasing height. Another dust layer about 1 km thick, and a higher dust free layer (upper shaded layer) are indicated by the $q^2\sigma$ profile. However, the 2359 GCT profile does not indicate a dust free layer below 23 km for as yet unexplained reasons.

Between 2345 and 2355 GCT, a sharp decrease of $q^2\sigma$ occurred between 21.2 and 21.5 km where $q^2\sigma$ was generally increasing with height. The rather sudden onset and abatement of this layer indicates a transitory pocket of dust-free air within a generally "dusty" layer.

Below the first dust-free layers of any profile, the profile of $q^2\sigma$ suggests the presence of dust. However, the lower boundary of the dust is not clearly defined. In the 2336 and 2337 GCT profiles, that boundary appears to be near 18 km. The next two profiles indicate a 20 km base to the dust. The following three profiles do not extend downward far enough to define where an increase in $q^2\sigma$ begins. The data taken between 2352 and 2357 GCT show some indication that the dust layer might begin near 18 km. The final profile indicates the base of the dust layer to be about 20 km.

Another feature of Fig. 2 cannot be easily ignored. There is a striking similarity of the shape of the profiles of the first two records, the next two, the next three and the next three. The last one is similar to the earlier profiles in the 15 to 20 km layer but different at higher altitudes. Each profile group appears to be characteristic of a five-minute period, after which, the shape of the profile changes and bears little resemblance to the previous one.

Low Altitude Analysis.--Usually most of the changes of scattering taking place in the lower levels of the atmosphere can be attributed to aerosols. This is particularly true for this series of laser firings. Records 422 through 429 were taken to examine the spatial distribution of aerosols within the boundary layer, without knowing what features would be found.

The spatial distribution of $q^2\sigma$ (obtained from Records 422 to 425 and 428) is shown in Fig. 3. This distribution has several features which would be expected in a convective regime. The horizontal and vertical dimensions of the cell of larger $q^2\sigma$ values are each about 1.2 km--a characteristic size for a fair weather cumulus cloud. The base is approximately 750 m above the sea surface which is within the accuracy of the cloud base height estimate made by the weather observer. It also agrees with the convective condensation level (650 m) computed from the radiosonde twelve hours previous.

The data do not indicate a visible cloud. The gradient of $q^2\sigma$ along any radial is not large enough to suggest cloud droplets. However the maximum values may be enhanced somewhat by aerosols (dust or salt particles) which were wetted by attracted moisture, but had not formed drops. No records are available which specifically describe the visible character of the air into which the laser was fired.

The distribution appears to have two towers (denoted A and B in Fig. 3) which may be the result of thermals rising, transporting particles upward, but tilted in response to wind shear. Malkus (ref. 11) found that the slope of cumulus towers was a function of the wind shear, the vertical velocity within the cloud and the horizontal frictional forces between the cloud and its environment. Using the wind shear from the available radiosonde (~ - 3m/sec/km), a friction coefficient of 2/km, and the slope of the towers gives vertical velocities ~3m/sec for tower A and 1.5 m/sec for tower B. These velocities are also characteristic of cumulus clouds, but for a convective tower with no condensed water, they are rather large. A larger value for the friction coefficient would give smaller velocities. The velocities are at least consistent with the observation, as tower A reaches a higher altitude than does tower B.

If the aerosol content were horizontally stratified as indicated by the vertical probe, the values of $q^2\sigma$ along the slant range probes should be lower than they are since the optical path length for a given range would be greater than in the vertical. Consequently the absolute values of $q^2\sigma$ should be even higher than indicated along the slant range. Thus it is even more evident that a cluster of aerosols was sampled.

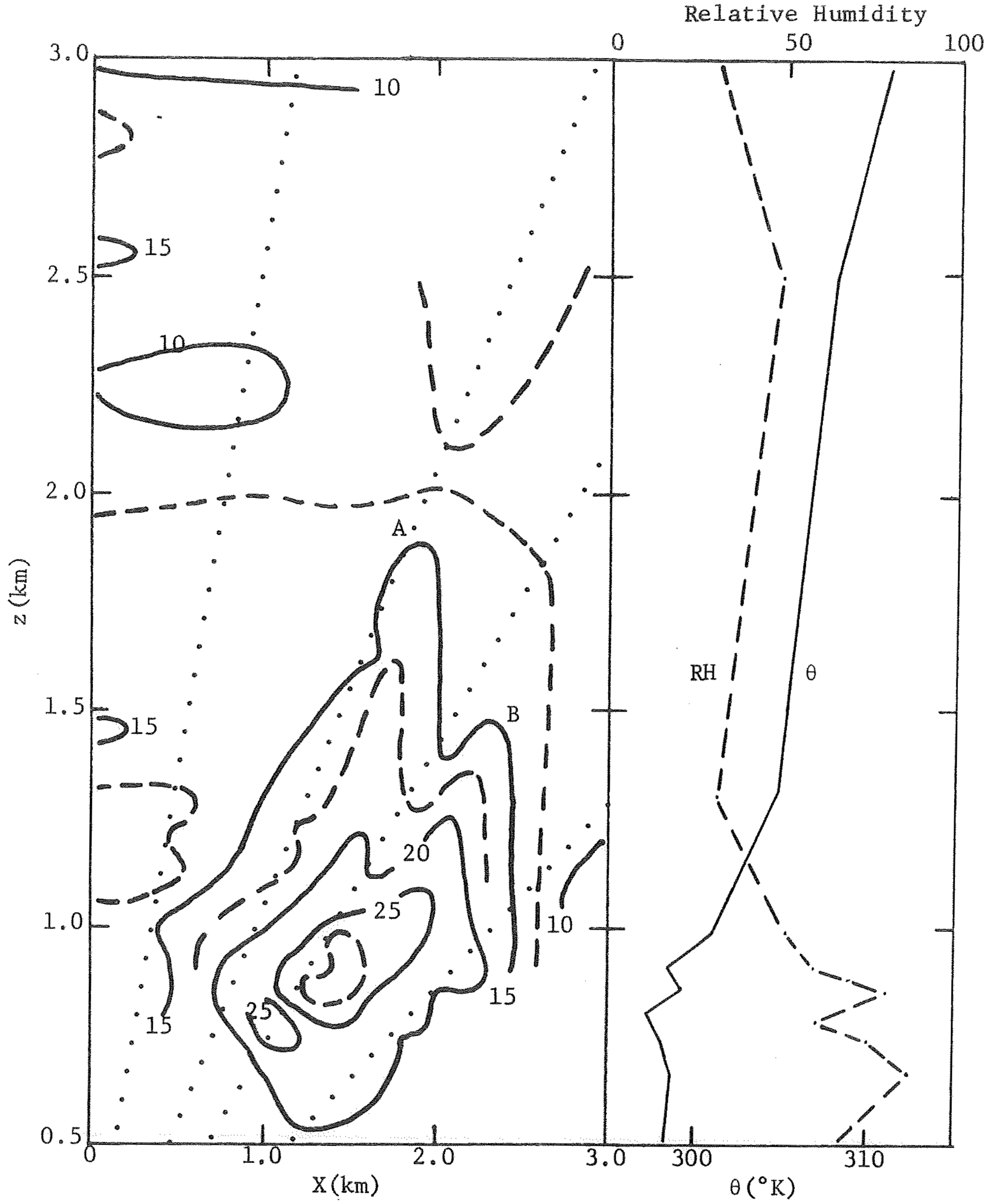

Figure 3. Space cross section of $q^2\sigma$ in planetary boundary layer, neglecting average wind. Data taken from 0007 to 0017 GCT, 27 June. Dotted lines indicate axis of laser beam. Potential temperature and relative humidity profiles from USCG Cutter ROCKAWAY, 1200 GCT, 26 June.

No attempt to normalize the values was made, or could be logically made.

The foregoing analysis is quite tentative as certain assumptions were made that may not be true. First it was assumed that the laser was always pointed along the same azimuth angle relative to the earth. This implies that the ship's heading was constant. Secondly it is assumed that all probes had a common origin--meaning that the ship's geographic position did not change. The average drift velocity of the ship was however 1.0 to 1.5 knots. It is further implied, in performing the analysis, that the distribution of aerosols and water vapor did not substantially change over the time (10 min) required to obtain the data. Substantial changes of the visible portion of fair weather cumuli do take place over a comparable time. Additionally, visible clouds move at or near the speed of the wind at the layer in which they are imbedded.

Figure 4 shows another distribution of $q^2\sigma$ derived by assuming that the average wind relative to the ship in the lower 3-km layer was normal to the ship at 10 m/sec and was also parallel to the projection of the laser axis on the horizon plane. Also it was assumed that the aerosols move with the speed of wind relative to the ship. No detailed records were kept of the ship's heading or the laser azimuth angle to verify those assumptions.

The convective towers identified in Fig. 3 are also apparent in this figure. However, they appear to be separate entities here and do not have a common source. The separation of the centers is 1.5 to 2.0 km with a minimum in $q^2\sigma$ between them. Tower A is slightly wider (1.7 km) and tower B is narrower (0.8 km) than before, but those dimensions are still reasonable for small cumulus clouds. The tilt of tower A with height is not much different than before, which means that a vertical velocity of ~3 m/sec is still valid. However, tower B appears to tilt more which implies that its vertical velocity should be less than the 1.5 m/sec previously given for it.

The estimates of vertical velocity present some incongruities with the observed aerosol distribution. In convective motion, one expects the greatest amount of convergence to take place with the stronger updraft. If the convective motion began with a uniform aerosol distribution, the greatest aerosol concentration ($q^2\sigma$) should occur with the stronger updraft. That is not the case here, so it must be assumed that the initial aerosol distribution was not homogeneous. It may also be the case that tower B is still in a developing stage whereas tower A has reached a more mature stage.

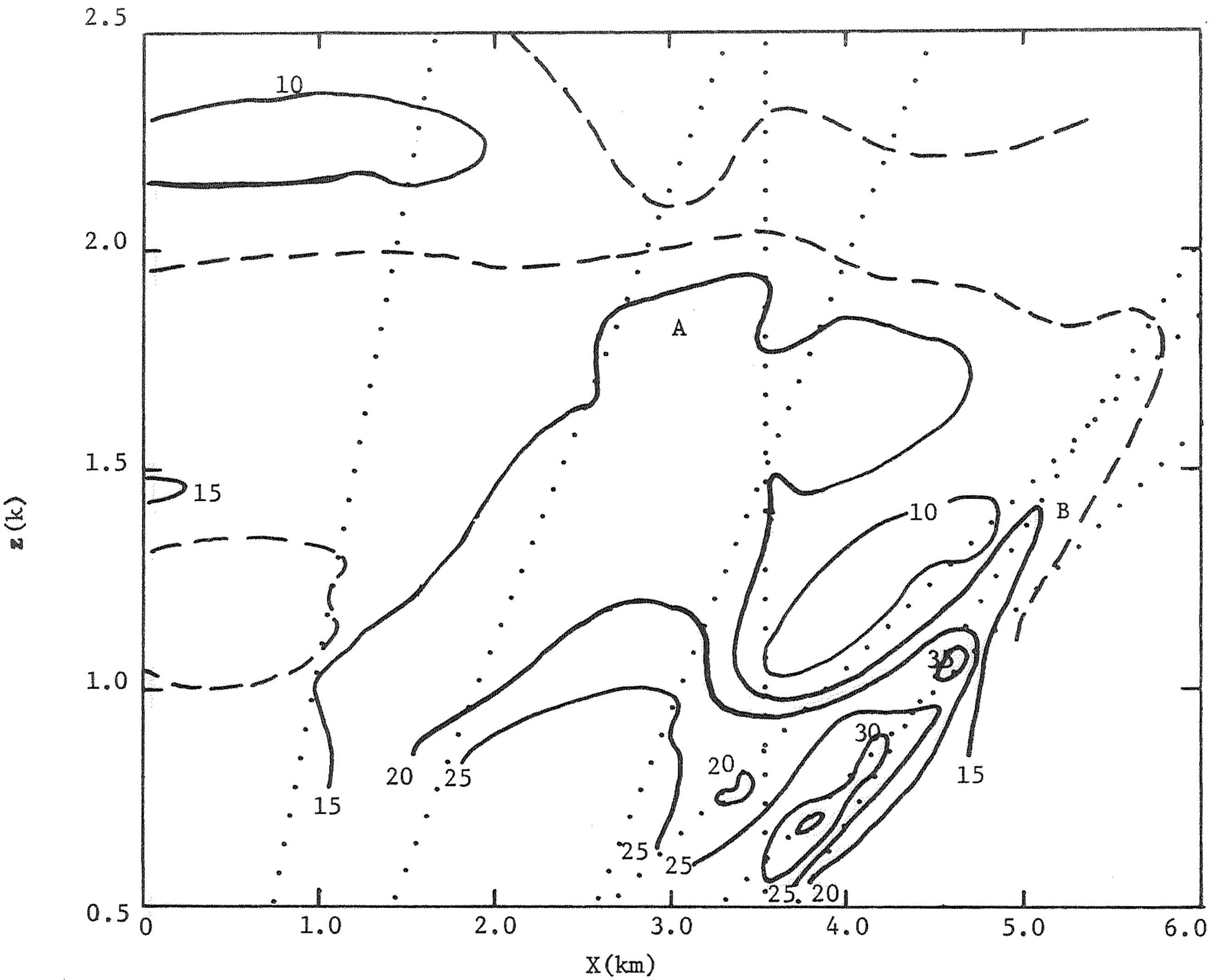

Figure 4. Space cross section of $q^2\sigma$ in planetary boundary layer accounting for an average wind. Data taken from 0007 to 0019 GCT, 27 June. Dotted lines indicate axis of laser beam.

Meteorological Data Analysis

The available radiosonde data are given in terms of temperature, pressure, and relative humidity or dew-point depression. As the laser data are in terms of range, the radiosonde data were first interpreted in terms of altitude, instead of pressure by integrating the hydrostatic equation.

Stable layers of the atmosphere inhibit the vertical transport of energy and momentum. As atmospheric aerosols are principally carried by the air motion, these stable layers also inhibit the transfer of aerosols. By the same reasoning, one would anticipate a rather uniform distribution of aerosols in unstable or only slight stable layer. The best indicator of static stability in the atmosphere is the vertical gradient of the potential temperature, θ, where θ is defined by

$$\theta = T\left(\frac{1000}{p}\right)^{R/c_p}$$

and

T is the temperature in degrees Kelvin,

p is the pressure in millibars,

R is the gas constant for dry air, and

c_p is the specific heat at constant pressure for dry air.

When $\frac{\partial \theta}{\partial z}$ is positive, the atmospheric layer is considered stable and vice versa.

In cases where the dew-point temperature depression was given, the relative humidity was calculated. Temperature, potential temperature and relative humidity were then plotted as a function of altitude for each radiosonde ascent.

Before any laser data were available, route cross sections of θ were constructed from the ADVANCE II radiosonde data. These cross sections were divided into the Wilmington to BOMEX area portion and the Paramaribo to the Amazon River portion. They were further divided into altitudes ranges of 0 to 15 km and 15 to 30 km. Those ranges were chosen to represent the tropospheric and lower stratospheric regions.

By constructing these cross sections, three benefits were derived. First, the analyst was familiarized with atmospheric thermal structure during the cruise. Second, stable and unstable layers could be identified. Finally, the longer term variation in stratification could be easily visualized. The latter two benefits also give the analyst the opportunity to locate, a priori, the regions of the atmosphere where significant laser radar returns would be expected. Additionally, a first approximation to atmospheric structure could be made for those laser firings which were unaccompanied by radiosonde ascents. It must be recognized however, that the cross sections, as well as other meteorological data, reflect only the larger scales of motion and stratification and do not reflect the short term variations which are reflected in the laser data.

The surface to 15-km altitude route cross section for the Paramaribo to the Equator cruise by is shown in Fig. 5. One of the most apparent features is that the vertical separation of the 340°K and 345°K θ-surfaces is greater than any other adjacent surfaces. That layer is less stable and should be identifiable in the laser data as a layer having a relatively constant decrease of returned signal since the aerosols should be well mixed. Slightly south of the intertropical convergence zone (ITCZ), the 345°K surface is lifted rather rapidly. A very stable layer, possibly a tropopause, is formed, between 13 and 15 km. (Other data indicate the tropical tropopause to be above 15 km further north). A rapid warming of the 10 to 15-km layer took place on 8 July. The cause of that warming has not been established. This warming and increase of stability should also be identifiable in the laser data.

In the middle levels (3 to 10 km) the θ-surfaces are rather uniform, with the exception of a disturbance from 4 July to 6 July. The lowering, raising and lowering of the θ-surfaces during this period are indicative of the transitory weather system which was encountered.

Below 3 km, the major feature is the departure of the 300°K surface from the nearly level 305°K and 310°K surfaces. During local daytime hours (4 hours from GCT) unstable layers due to surface heating resulted on 3 July and 6 July. Insufficient data during daytime hours prohibited positive identification of similar layers on other days. The only feature coincident with the ITCZ at any level is the lack of a 300°K surface. The lowest 1.5 km was therefore only slightly stable, as a result of the convergence and lifting in the low levels and a pressure reduction.

The ITCZ does not maintain a fixed position even over a period of a day. It wanders in response to the dynamical processes of the air in the northern and southern hemisphere. It does not, in itself, delineate air mass characteristics as does a front in mid-latitudes, nor does it prevent air parcels from passing through it. It is simply the surface low pressure axis, separating the circulation of the subtropical high pressure systems of either hemisphere.

The location of the ITCZ was determined independent of the cross section analysis, laser data or particle sampling data. The 0000 and

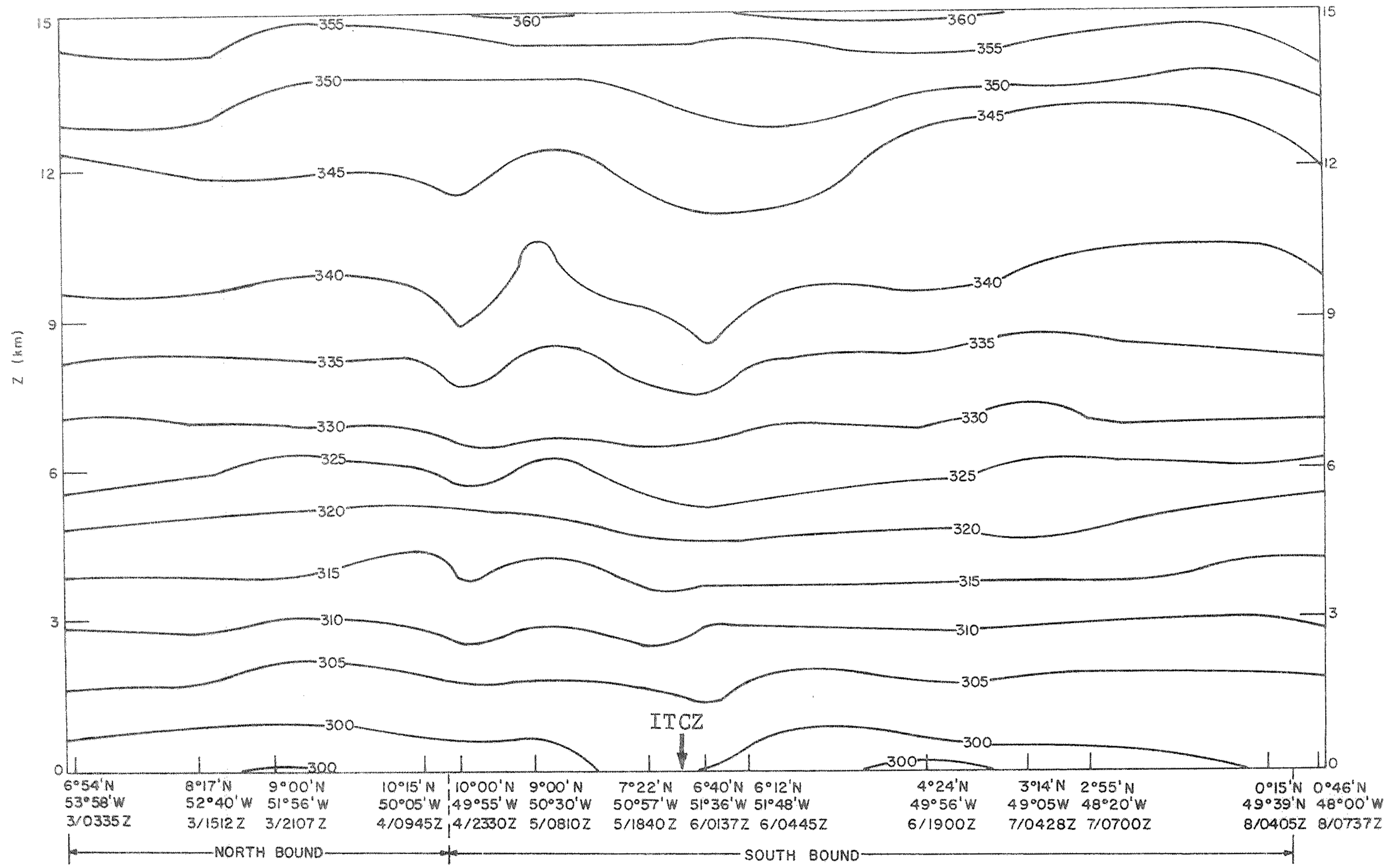

Figure 5. Route cross section of potential temperature (θ) constructed from radiosonde released from S. S. ADVANCE II at position and time indicated. Intertropical convergence zone (ITCZ) position determined from trajectory analysis (Fig. 6).

1200 GCT "TOE" (Top of Ekman layer, ~3000 ft) streamline analyses obtained from NHRL were used to determine the trajectories of air parcels arriving at the ship's location at particular times.

The trajectories (Fig. 6) are only approximate. Their uncertainty increases with distance away from the cruise track. A col region was located near 12°N, 25°W, on 30 June and 1 July which further increases the uncertainties in the northern hemisphere trajectories. There were only a few wind reports at this level in the Equatorial and South Atlantic areas on which to base the analysis. Despite these limitations, the trajectories do show that there is a definite change in the source region of the air reaching the ship between 1500 GCT, 5 July and 0000 GCT, 6 July. The ITCZ is considered to lie between the positions of the ship at these times.

The primary source of dust in the lower atmosphere in the trade wind latitudes is the Sahara Desert. There high surface winds and vertical mixing raise the dust and distribute it throughout the first 5 km. Persistent easterly winds throughout that layer transport the dust across the South Atlantic Ocean. As indicated by the air trajectories, several days are required for transit. During transit some particles coagulate and settle to lower levels. The falling upper level particles partly replenish the fallout from lower levels. The smaller particles remain aloft since their terminal fall velocities are quite small. Consequently larger particles are more likely to be found near the earth's surface as well as higher concentrations. All sizes are subject to washout by precipitation and to vertical transport by deep convective clouds.

In the lower levels (~1 km), it appears that there should be many more dust particles in the region to the north of the ITCZ. Furthermore, the concentration of particles should increase as the ITCZ is approached along the cruise track since the more northern trajectory has a longer over water fetch; it does not eminate from Africa directly, and precipitation in the col area may have depleted the dust concentration. Except for local showers, the more southerly trajectory (but still north of the ITCZ) has not passed through a known organized precipitation system and has a slightly more direct trajectory from Africa.

To the south of the ITCZ, the low levels of the air should be relatively dust free. Trajectories there have their origin in the South Atlantic, away from dust sources. Some dust may be present however due to gravitational settling of higher level dust. The trajectories for the 500-mb (~5.5 km) flow in Fig. 7 show a more direct latitudinal flow from over Africa and very little evidence of a narrow convergence zone like that found at lower levels.

Scientists from NASA and RTI who were aboard the ship have verified that they observed a substantial change in the visual characteristics of the air took place in the vicinity of the ITCZ located by the trajectory analysis.

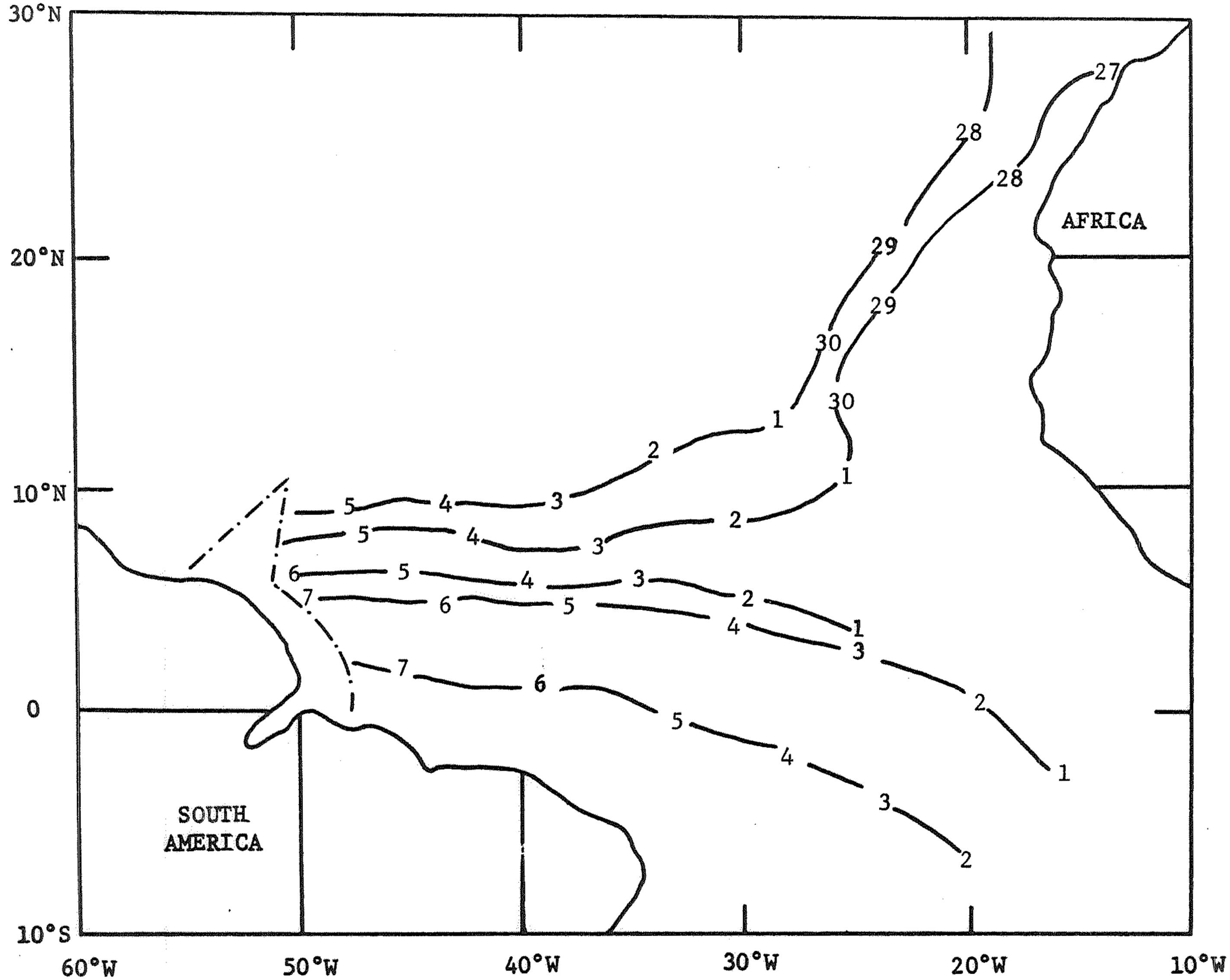

Figure 6. Trajectories of air parcels at ~1 km altitude arriving at S. S. ADVANCE II position. 0000 GCT parcel position indicated by date in trajectory.

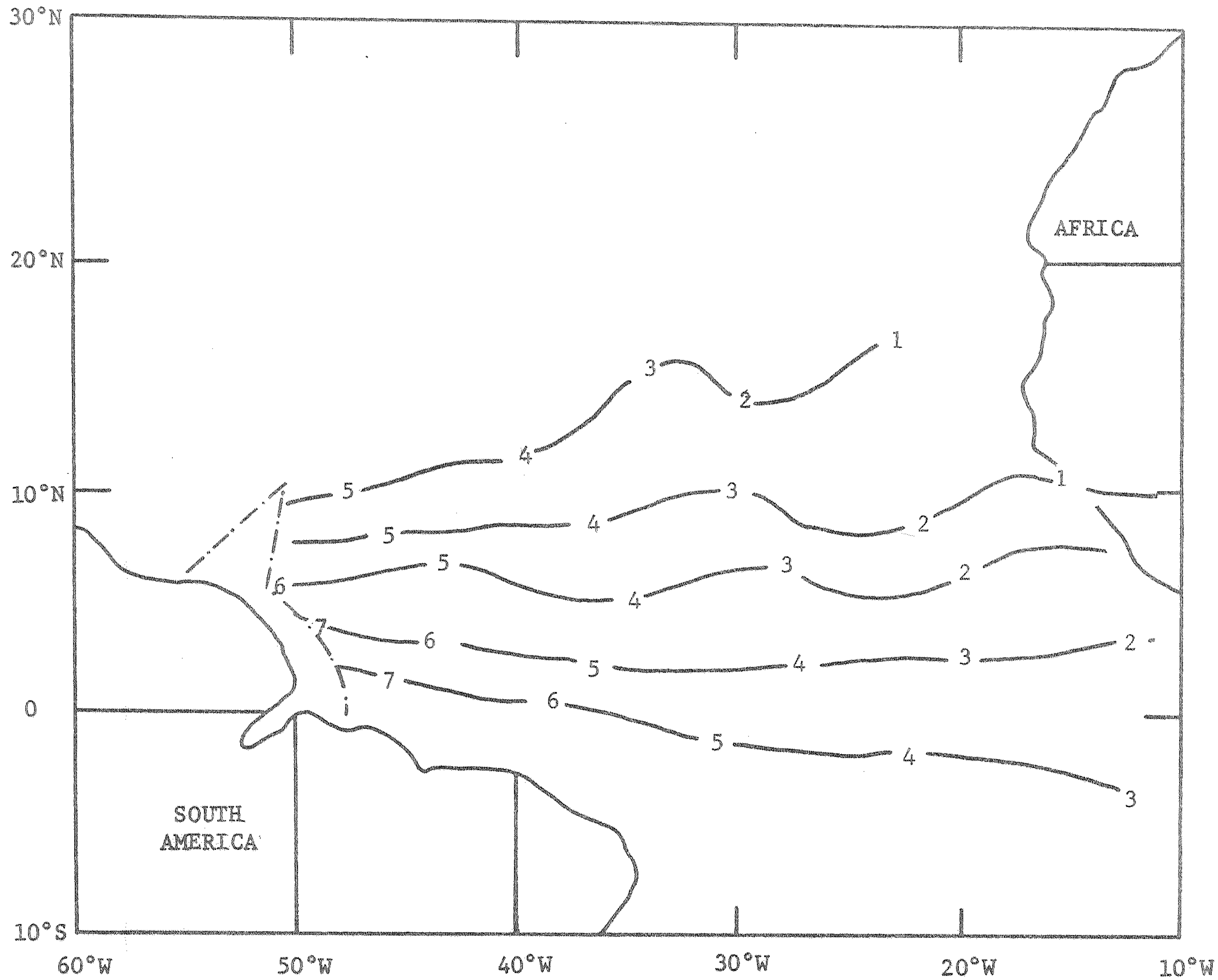

Figure 7. Trajectories of air parcels at 500 mb (~5.5 km) arriving at S. S. ADVANCE II position. 0000 GCT parcel position indicated by date in trajectory.

Distributions of particle number density as measured aboard the ADVANCE II are shown in Fig. 8 . To the north of the ITCZ no appreciable latitudinal gradient of number density was noted. There is however an order of magnitude reduction in the number density of all but the smallest (0.5μ) diameter particles as the ITCZ was crossed. The reduction in particulates was due to the change source regions of dust and the reduction of salt nuclei production by virtue of the significantly calmer seas encountered. The increase in the number of small (0.5μ) particles to the south of the convergence zone is possibly due to a bias in the analysis. As there were significantly fewer large particles, the number of small particles becomes more apparent in an analysis.

Further south, the number of 1.5 to 2.0μ diameter particles increases. At that time, the ship was close to the coast of Brazil and the air there was under the influence of a different, more localized circulation system. These two factors probably account for the observed increase.

In the process of reviewing the meteorological and unreduced laser data, RTI and NASA scientists found numerous instances of correlation and non-correlation of the two data sets in all portions of the cruise. Enhanced laser returns were found at or very near to heights where the radiosonde signal was distorted. The cause of the fluctuations was not resolved, but the phenomenon cannot be lightly excused as coincidence.

Except in the BOMEX area, the trade wind inversion was not consistently found in either set of data. The subsidence necessary to maintain the inversion is a maximum to the southeast of the subtropical high pressure center, and decreases to the west and north. The BOMEX area portion of the cruise was the nearest approach to the region of maximum subsidence.

In the stratosphere, the dust layer near 20 km was generally found to be increasing in height with decreasing latitude. Day-to-day changes in its altitude have not been documented.

A haze layer, first mistaken for a cirro-stratus cloud layer, was observed on 4 July and persisted until 6 July. Cursory examination of unreduced laser photographs do not give any indication of this layer which was estimated by the weather observed to be at 14,000 ft.

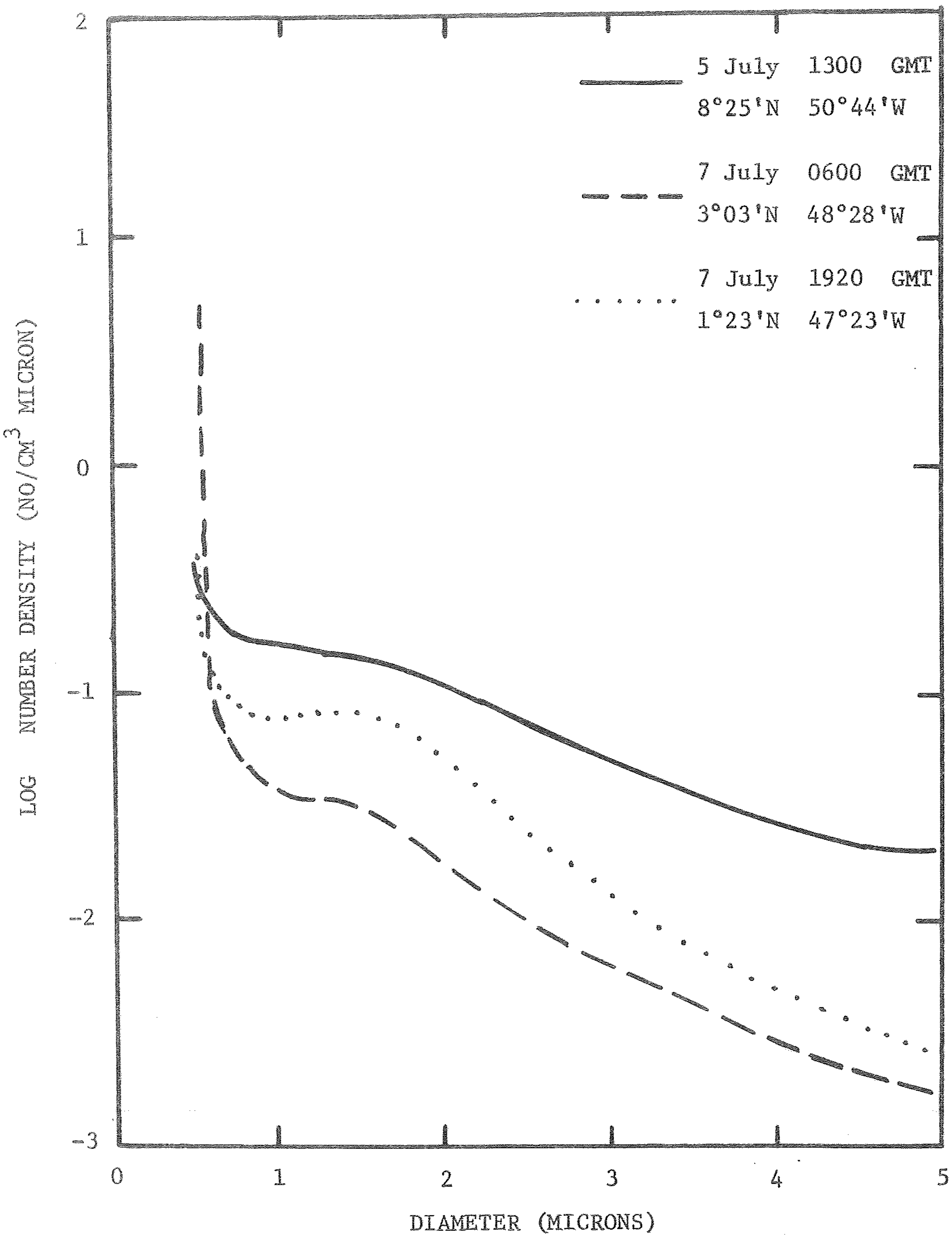

Figure 8. Number density of particulates in vicinity of ITCZ.

SUMMARY

Although the data from only one sequence of laser firings were analyzed, most of the objectives of the research were realized. Meteorological data were collected, and analyzed for the broad scale features which should relate to all of the laser data collected. The ITCZ was located by air trajectory analysis. The observed particle number density distributions showed a sharp decrease in the number of large particles to the south of the ITCZ.

The analysis of one sequence of laser data confirmed the existence of dust in the 15 to 25-km range. A wide variability in the energy returned to the laser, indicating a large variation in lower level aerosol distribution was noted. Additionally, a change of the character of laser profiles in this region over a five-minute period was noted but not explained.

In low altitudes, the laser data indicated a distribution of aerosols on the space scale of small dry convective towers. Estimate vertical velocities within the towers ranged from 3 to 1.5 m/sec.

Meteorological data were available on a broad scale, but there were no laser data for it. Laser data with no current meteorological data were available. There was only a limited time for analysis. Nevertheless, some features of the marine atmosphere were identified but have not been fully interpreted. Preliminary indications are that the laser can be used as an effective remote sensor in the marine environment, but still, precise meteorological measurements on the time scale of the interval between laser firings are desirable to assist in the development of a signature bank for laser profiles as "ground truth data".

RECOMMENDATIONS FOR FUTURE WORK

There are many more laser data records to be examined in terms of the physical and dynamical processes of the marine atmosphere. The study of only one sequence of data has shown that features of the atmospheric boundary layer may be identifiable in the data. Dust in the region of 20 km was also identified.

Much work remains to be done to correlate the long term changes in laser signals with the broad scale changes which occurred in the atmosphere. The first step in such a study should be to construct composite profiles of laser data as a function of time or space.

These data should be analyzed concurrently with the meteorological cross sections already derived to determine

(1) the slope of the 20 km dust layer,

(2) the influence of meteorological changes upon changes of the dust layer,

(3) the rise and fall of θ-surfaces and their affects upon aerosol concentration, and

(4) the laser signature of the haze layer reported in weather observations.

Changes over a period of an hour or so may be identified particularly in the BOMEX area where data were taken frequently. In that area, particle sampling was conducted at various altitudes. There the vertical distribution of aerosols can be used to further refine the laser data and perhaps inference of aerosol distributions outside of BOMEX area can be made.

Finally, the short term variation (1 to 30 min) of atmospheric properties can be further investigated at all altitudes of interest. There are more cases where the atmospheric boundary layer was probed by the same technique as reported in this paper. The success of finding an identifiable feature necessitates that all of those cases be investigated. Even more upper troposphere-lower stratosphere data are available, and the short term changes there should be investigated. The instance where enhanced laser returns were received from the same altitudes where the radiosonde signal was distorted should also be investigated.

When future operations are carried out in a marine environment, records should be made of the ship heading, ship speed, and relative wind velocity during periods of laser firings. When probing the marine boundary layer, observations of cloud types, amounts, and bases and tops and obstructions to visibility should be made before, during, and after laser operations to assist in post analysis.

REFERENCES

1. Johnson, W. B.: Lidar Applications in Air Pollution Research and Control. J. Air Poll. Control Assoc., vol. 19, no. 3, March 1969, pp. 176-180.

2. Fernald, F. G., et al.: Analytical and Experimental Investigations of Lidar for Meteorological Applications (PMR-MR-68-2 DDC No. AD 829 082) Stanford Res. Inst., September 1967.

3. Grams, G.; and Fiocco, G.: Stratospheric Aerosol Layer During 1964 and 1965. J. Geophys. Res., vol. 72, no. 14, pp. 3523-3542.

4. Lawrence, J. D., Jr.; McCormick, M. P.; Melfi, S. H.; and Woodman, D.P.: Optical Radar Studies of the Atmosphere. Paper presented at Fifth Symposium on Remote Sensing of Environment (Ann Arbor, Michigan), April 1968.

5. Collis, R. T. H.; and Ligda, M. G. H.: Note on Lidar Observations of Particulate Matter in the Stratosphere. J. Atmos. Sci., vol. 23, no. 2, March 1966, pp. 255-257.

6. Prospero, J. M.: Atmospheric Dust Studies on Barbados. Bull. Am. Meteoro. Soc., vol. 49, no. 6, June 1968, pp. 645-652.

7. Elterman, L.; Wexler, R.; and Chang, D. T.: Features of Tropospheric and Stratospheric Dust. Appl. Opt., vol. 8, no. 5, May 1969, pp. 893-903.

8. Junge, C. E.; Changon, C. W.; and Manson, J. E.: Stratospheric Aerosols. J. Meteoro., vol. 18, no. 1, February 1961, pp. 81-108.

9. Rosen, J. M.: Simultaneous Dust and Ozone Soundings Over North and Central America. J. Geophys. Res., vol. 73, no. 2, January 1968, pp. 479-486.

10. Lawrence, J. D., Jr.; Crownfield, F. R., Jr.; and McCormick, M. P.: Optical Radar Measurements of the Atmosphere. NASA CR-729, 1967.

11. Malkus, J. S.: The Slopes of Cumulus Clouds in Relation to External Wind Shear. Quart. J. Roy. Meteorol. Soc., vol. 78, 1952, pp. 530-542.